Structural Studies of Duck δ1 and δ2 Crystallin Suggest Conformational Changes Occur during Catalysis[†,‡]

Liliana M. Sampaleanu,[§,||] François Vallée,[§] Christine Slingsby,[⊥] and P. Lynne Howell*[,§,||]

Structural Biology and Biochemistry, Research Institute, Hospital for Sick Children, 555 University Avenue, Toronto, Ontario M5G 1X8, Canada, Department of Biochemistry, Faculty of Medicine, University of Toronto, Toronto, Ontario M5S 1A8, Canada, and Department of Crystallography, Birkbeck College, Malet Street, London WC1E 7HX, U.K.

Received September 27, 2000; Revised Manuscript Received December 18, 2000

ABSTRACT: Duck δ1 and δ2 crystallin are 94% identical in amino acid sequence, and while δ2 crystallin is the duck orthologue of argininosuccinate lyase (ASL) and catalyzes the reversible breakdown of argininosuccinate to arginine and fumarate, the δ1 isoform is enzymatically inactive. The crystal structures of wild type duck δ1 and δ2 crystallin have been solved at 2.2 and 2.3 Å resolution, respectively, and the refinement of the turkey δ1 crystallin has been completed. These structures have been compared with two mutant duck δ2 crystallin structures. Conformational changes were observed in two regions of the N-terminal domain with intraspecies differences between the active and inactive isoforms localized to residues 23−32 and both intra- and interspecies differences localized to the loop of residues 74−89. As the residues implicated in the catalytic mechanism of δ2/ASL are all conserved in δ1, the amino acid substitutions in these two regions are hypothesized to be critical for substrate binding. A sulfate anion was found in the active site of duck δ1 crystallin. This anion, which appears to mimic the fumarate moiety of the argininosuccinate substrate, induces a rigid body movement in domain 3 and a conformational change in the loop of residues 280−290, which together would sequester the substrate from the solvent. The duck δ1 crystallin structure suggests that Ser 281, a residue strictly conserved in all members of the superfamily, could be the catalytic acid in the δ2 crystallin/ASL enzymatic mechanism.

Crystallins are the major proteins in vertebrate lenses, representing 80−90% of the total water-soluble proteins in this organelle (*1*). The refractive properties of the lens originate in the gradual accumulation of crystallins in the concentric layers of the fiber cells, while the transparency of the lens is acquired through the short-range interactions established between crystallins (*2*). In vertebrates, crystallins can be divided in two classes, the ubiquitous crystallins (α, *β*, and *γ*) and the taxon-specific crystallins (*δ*, *ϵ*, *ζ*, *η*, *λ*, *μ*, *ρ*, *τ*, and S) (*3*, *4*). The discovery that crystallins are multifunctional proteins that have been recruited from a wide variety of proteins, from small heat shock proteins to housekeeping enzymes, led to the development of the gene sharing or gene recruitment hypothesis (*3*, *4*). According to this theory, no gene duplication is required prior to recruitment of a protein to a refractive role in the lens. Following the recruitment step, gene duplication may occur with the subsequent specialization of the duplicated gene (*5*). Recent studies indicate that overexpression of various metabolic enzymes also occurs in a taxon-specific manner in the corneal epithelial cells of vertebrates (bovine BCP 54 and chicken δ1 crystallin) and invertebrates (squid S crystallin and drosocrystallin) (*6*), suggesting that gene sharing is a more widespread phenomenon (*7*). Indeed, gene sharing has recently been suggested to be an important factor in eye morphogenesis and evolution, contributing to the eye's diversity and complexity (*8*).

δ crystallin is the major soluble protein in the eye lenses of birds and terrestrial reptiles. This crystallin was recruited from the housekeeping enzyme argininosuccinate lyase (ASL)[1] (*5*, *9*), a cytosolic enzyme that catalyzes the reversible breakdown of argininosuccinate to arginine and fumarate. The gene recruitment step, which was followed by gene duplication, resulted in two proteins, δ1 and δ2 crystallin. In ducks, the amino acid sequences of the δ1 and δ2 isoforms (dδc1 and dδc2, respectively) are 94% identical, and the sequences of dδc1 and dδc2 are 69% and 71% identical to that of human ASL, respectively (*5*, *10*). During evolution, only the δ2 isoform has retained enzymatic activity and is

[†] Supported by a grant from the CIHR of Canada to P.L.H. and by a multiuser maintenance grant from the CIHR and NSERC of Canada for beamline X8C at the NSLS.

[‡] The coordinates and structure factors have been deposited in the Protein Data Bank, as entries 1HY0, 1HY1, and 1I0A for dδc1, dδc2, and tδc1, respectively.

* To whom correspondence should be addressed. E-mail: howell@sickkids.on.ca. Telephone: (416) 813-5378. Fax: (416) 813-5022.

[§] Hospital for Sick Children.

[||] University of Toronto.

[⊥] Birkbeck College.

[1] Abbreviations: ASL, argininosuccinate lyase; dδc1, duck δ1 crystallin; dδc2, duck δ2 crystallin; tδc1, turkey δ1 crystallin; H162N dδc2, duck δ2 crystallin His 162* to Asn mutant; H91N dδc2, duck δ2 crystallin His 91* to Asn mutant; rms deviation, root-mean-square deviation; X_i, residue *X* belonging to monomer i, where i is A, B, C, or D. The amino acid numbering used throughout this paper corresponds to dδc1/ASL. dδc2 has a two-residue insertion at amino acid 5. *The name of the dδc2 mutants was maintained in the dδc2 numbering scheme (shifted by two) to facilitate referencing to previously published papers.

10.1021/bi002272k CCC: $20.00
Published on Web 02/02/2001

the duck orthologue of ASL in non-lens tissues (*11*, *12*). δ1 crystallin is assumed to have become more specialized for the structural role in the eye lens and in the process has lost its catalytic function (*13*−*15*). The loss of enzymatic activity in δ1 crystallin is the consequence of the amino acid differences (27 of 466) between the two isoforms. Duck δ1 and δ2 crystallin therefore offer a unique system for investigating the catalytic mechanism of ASL.

ASL and δ crystallin are members of a superfamily of enzymes that are active as homotetramers and catalyze similar reactions in which a C_α−N or C_α−O bond is cleaved with the subsequent release of fumarate as one of the products. Members of the superfamily include class II fumarase (*16*), aspartase (*17*), adenylosuccinate lyase (*18*), and 3-carboxy-*cis*,*cis*-muconate lactonizing (CMLE) enzyme (*19*). Although the level of overall amino acid sequence homology between these proteins is low (20−30%), there are three highly conserved regions that are remote from each other in the monomer structure but cluster together in the tetramer to form the four active sites (*20*−*23*). The location of the active site was confirmed with the structure determination of various superfamily members with bound inhibitors, substrate analogues, or substrates (*24*−*27*).

Structural and biochemical studies (*28*, *29*) as well as site-directed mutagenesis data (*30*) have suggested that His 160, directly (*20*, *22*) or via a water molecule (*26*), is responsible for proton abstraction (base catalysis), while Lys 287 has been proposed to stabilize the carbanion intermediate (*20*, *21*). Although site-directed mutagenesis experiments of duck δ2 crystallin (*31*) and the structure of an inactive duck δ2 crystallin mutant with substrate bound (*24*) have confirmed the role of a number of residues in the active site, a viable candidate for the catalytic acid has yet to be identified and questions remain about the role of His 160, as this residue is not conserved across the superfamily.

Since all the residues known or suggested to be involved directly in catalysis are conserved between δ1 and δ2 crystallin, the sequence variations between the two must replace crucial substrate binding residues or produce conformational changes that prevent substrate binding and/or catalysis in δ1 crystallin. Most of the amino acid differences (17 of 27) are clustered in the first structural domain comprised of residues 1−112. Biochemical and structural data have shown the importance of some of these residues (*15*, *22*, *31*) and have demonstrated the crucial role that the entire domain 1 plays in the recovery of catalytic activity by chimeric proteins of duck δ1 and δ2 crystallin (*32*). Significant conformational changes in domain 1 were also observed when comparing the turkey δ1 crystallin (tδc1) (*20*) and the H91N and H162N dδc2 structures (*22*, *24*).

The previous structural comparisons involved mutant duck δ2 and wild type turkey δ1 crystallin, and therefore, it could not be determined if the observed conformational variations were the result of intra- or interspecies differences. We report here the structure determinations of wild type duck δ1 and δ2 crystallins, the complete refinement of turkey δ1 crystallin, and structural comparisons of all available δ crystallin structures. The results of these studies show that distinct inter- and intraspecies conformational differences do exist and that they are localized to domain 1. A major conformational change in a loop of domain 2 and a rigid body movement in domain 3 are also observed in dδc1. These conformational changes are the result of a sulfate ion bound to dδc1, in a position that appears to mimic the fumarate moiety of argininosuccinate in the enzymatically active dδc2. The structural analyses suggest that Ser 281 could be the acid catalyst in the enzymatic mechanism of the dδc2/ASL superfamily.

MATERIALS AND METHODS

Expression and Purification of dδc1 and dδc2. The dδc1 expression vector (pET-17b-dδc1) was described previously (*32*). The dδc2 expression vector (pET-3d-dδc2) was a gift of W. E. O'Brien (Baylor College of Medicine, Houston, TX). The pET-17b-dδc1 and pET-3d-dδc2 plasmids were transformed into *Escherichia coli* BL21 (DE3) pLysS and the proteins expressed using a T7 polymerase system. The expression protocol was similar to that described previously for wild type dδc2 (*15*, *30*).

Purification of dδc1. Duck δ1 crystallin was purified using a three-step purification protocol. The first two steps involved anion exchange chromatography on a DEAE-cellulose (DE-53 Whattman) column. Initially, a linear gradient from 0 to 300 mM NaCl (500 mL) was used to elute the protein. The protein fractions that eluted between 50 and 100 mM NaCl were pooled and concentrated with a Biomax Ultrafree 15 mL concentrator (Millipore). The concentrated fractions were desalted by overnight dialysis at 4 °C. Samples were subsequently reloaded on the DEAE-cellulose column, and a finer linear gradient from 0 to 100 mM NaCl was used for elution. The peak protein fractions (at ∼70 mM NaCl) were pooled, concentrated, desalted, and analyzed on a SDS−PAGE gel and found to be ∼90% pure.

To obtain higher-purity protein samples, dδc1 was further purified by two alternative methods, chromatofocusing on a Mono-P FPLC column and affinity chromatography on an arginine−Sepharose column. Isochromatofocusing (*22*) resulted in a protein that was ∼98% pure. This protein fraction (sample A) was exchanged into 10 mM Tris-HCl (pH 7.5), 1 mM EDTA, and 1 mM DTT and stored at 4 °C. For the arginine−Sepharose 4B (Pharmacia Biotech) column purification, a stepwise gradient of 1, 2.5, 5, 7.5, 10, and 25 mM arginine was used for elution. The protein was eluted with 2.5 mM arginine and found by SDS−PAGE to be 98−99% pure (sample B).

Purification of dδc2. The purification protocol for dδc2 was similar to that described above for dδc1 except that the final purification step was achieved using gel filtration chromatography. Low-molecular weight contaminants were removed by loading the protein sample on a S-200 Sephacryl column (Pharmacia), with a gel bed height of 1 m and a total volume of 200 mL, and eluting the sample with 10 mM Tris-HCl (pH 7.5) and 1 mM EDTA at 4 °C. Fractions containing the highest-purity dδc2 (∼98%) were pooled and concentrated.

Crystallization, Data Collection, and Structure Determination. Wild type dδc1 (samples A and B) and dδc2 were crystallized at room temperature using the hanging drop vapor diffusion method (see Table 1 for crystallization conditions). Data were collected for both wild type dδc1 and dδc2 at the National Synchrotron Light Source (NSLS) (Brookhaven National Laboratory, Upton, NY) and subsequently processed using the DENZO/SCALEPACK software package (*33*) (Table 1).

Table 1: Crystallization, Data Collection, and Data Processing Statistics[a]

	dδc1, data set A[b]	dδc1, data set B[c]	dδc2
protein concentration (mg/mL)	8	6	20
precipitant (w/v)	14% PEG 550 MME	15% PEG 550 MME	14% PEG 2000 MME
additive	7 mM $ZnSO_4$	10 mM $ZnSO_4$	300 mM $MgCl_2$
buffer, pH	100 mM MES, 7.5	100 mM MES, 6.5	100 mM HEPES, 7.5
morphology	prism-like	prism-like	flat plates
average size (mm)	0.75 × 0.2 × 0.15	0.8 × 0.25 × 0.2	0.4 × 0.2 × 0.1
NSLS beam line, λ (Å)	X12C, 0.98	X8C, 1.0	X12C, 0.98
detector type	Brandeis 1K CCD	MAR 30 cm IP	Brandeis 1K CCD
space group	$P3_121$	$P3_121$	$P2_1$
cell dimensions	$a = b = 100.7$ Å, $c = 167.2$ Å, $\gamma = 120°$	$a = b = 100.6$ Å, $c = 168.0$ Å, $\gamma = 120°$	$a = 93.5$ Å, $b = 99.1$ Å, $c = 107.2$ Å, $\beta = 102.1°$
no. of molecules/asymmetric unit	2	2	4
resolution limits (Å)	20−2.8	20−2.2	20−2.3
no. of total reflections	84845	147604	277694
no. of unique reflections	28147	48769	79045
mean redundancy	3	3	3.5
completeness (%)	91.4 (89.5)[d]	96.4 (94.2)[d]	93.2 (92.1)[d]
average $I/\sigma(I)$	6.7	7.4	15.2
% reflections with $I > 2\sigma(I)$	57.9 (34.9)[d]	83.7 (63.7)[d]	74.1 (46.2)[d]
R_{sym}[e]	0.08 (0.34)[d]	0.08 (0.29)[d]	0.05 (0.22)[d]

[a] Turkey δ1 crystallin purification, crystallization, data collection, and processing have been reported previously (*20*). [b] Isochromatofocusing purified dδc1. [c] Arginine−Sepharose-purified dδc1. [d] Last resolution shell: 2.69−2.6 and 2.28−2.2 Å for the 2.6 and 2.2 Å dδc1 data, respectively, and 2.38−2.3 Å for dδc2. [e] $R_{sym} = \Sigma|I - \langle I\rangle|/\Sigma I$, where I is the measured intensity for symmetry-related reflections and $\langle I\rangle$ is the mean intensity for the reflection.

The structures of dδc1 and dδc2 were determined by molecular replacement using the program AMoRe (*34*) and a monomer of the H110N dδc2 mutant (M. A. Turner and P. L. Howell, unpublished results) as the search model. Correlation coefficients of 0.49 and 0.43 and *R*-factors of 0.39 and 0.30 were obtained for dδc1 and dδc2, respectively. For dδc1, data set A (from protein sample A) was used to determine the structure and for initial refinement. The phases were subsequently extended to 2.2 Å using data set B (protein sample B).

Refinement and Model Building. The models were refined using the program CNS (*35*) with a maximum likelihood target function (*36*, *37*), a flat bulk solvent correction (*38*), and no low-resolution or σ cutoff applied to the data. Ten percent of the reflections were randomly selected to compute an R_{free} for cross-validation of the model (*36*). Each refinement step consisted of torsion angle simulated annealing (*39*), grouped and individual *B*-factor refinement, and the subsequent calculation of σ_a weighted $2|F_o| - |F_c|$ and $|F_o| - |F_c|$ electron density maps (*40*, *41*). These maps were then used to correct the models by manual rebuilding in TURBO-FRODO (*42*).

Refinement of the Wild Type dδc1 and dδc2 Structures. Noncrystallographic symmetry restraints were applied initially and gradually relaxed during the refinement. A cis peptide was modeled between Ser 319 and Thr 320 in all monomers of both structures. Water molecules with proper hydrogen bonding coordination and electron densities higher than 1σ on $2|F_o| - |F_c|$ and 2.5σ on $|F_o| - |F_c|$ σ_a weighted maps were progressively introduced while monitoring the decrease in R_{free} (Table 2). For dδc1, a sulfate anion was located in the σ_a weighted $|F_o| - |F_c|$ omit maps and modeled into the active sites.

Refinement of the Wild Type tδc1 Structure. The previously reported model of turkey δ1 crystallin (*20*) did not contain any solvent molecules. After a small number of C_α backbone corrections were made and several side chain rotamer conformations were changed, the corrected model was further refined using CNS. Noncrystallographic symmetry restraints were applied initially and gradually relaxed. These corrections, together with water molecule addition, decreased the R_{cryst} and R_{free} values from 20.2% and 26.2% to 15.7% and 21.3%, respectively.

Table 2: Summary of the Final Model Refinement Statistics

	dδc1 (set B)	dδc2	tδc1
resolution range (Å)	20−2.2	20−2.3	35−2.5
R_{cryst} (%)[a]	19.0	20.8	15.7
R_{free} (%)[b]	23.3	26.0	21.3
no. of reflections used in the refinement	47139	73580	66791
no. of reflections used to compute R_{free}	4749	7436	6651
no. of non-hydrogen atoms			
protein	6914	13921	13679
solvent	516	655	588
sulfate	10		
mean *B*-factor (Å^2)			
protein	31	33	41
per monomer (A/B or A/B/C/D)	28/32	32/36/32/32	42/42/42/38
per domain			
domain 1	35/43	33/42/56/54	42/56/48/56
domain 2	22/24	24/28/23/23	34/32/34/31
domain 3	36/42	50/49/33/35	62/53/57/42
solvent	37	33	47
sulfate	23		
rms deviation from ideal values			
bond lengths (Å)	0.008	0.006	0.005
bond angles (deg)	1.3	1.1	1.1
dihedral angles (deg)	18.8	18.9	18.9
improper angles (deg)	0.88	0.8	0.78
Ramachandran plot (% residues in most favored regions	93.4[c]	92.9[c]	92.8[c]

[a] $R_{cryst} = \Sigma(|F_o| - |F_c|)/\Sigma|F_o|$. [b] $R_{free} = \Sigma(|F_{os}| - |F_{cs}|)/\Sigma|F_{os}|$, where "s" refers to a subset of data not used in the refinement, representing 10% of the total number of observations. [c] No residues were found in the disallowed regions of the Ramachandran plots.

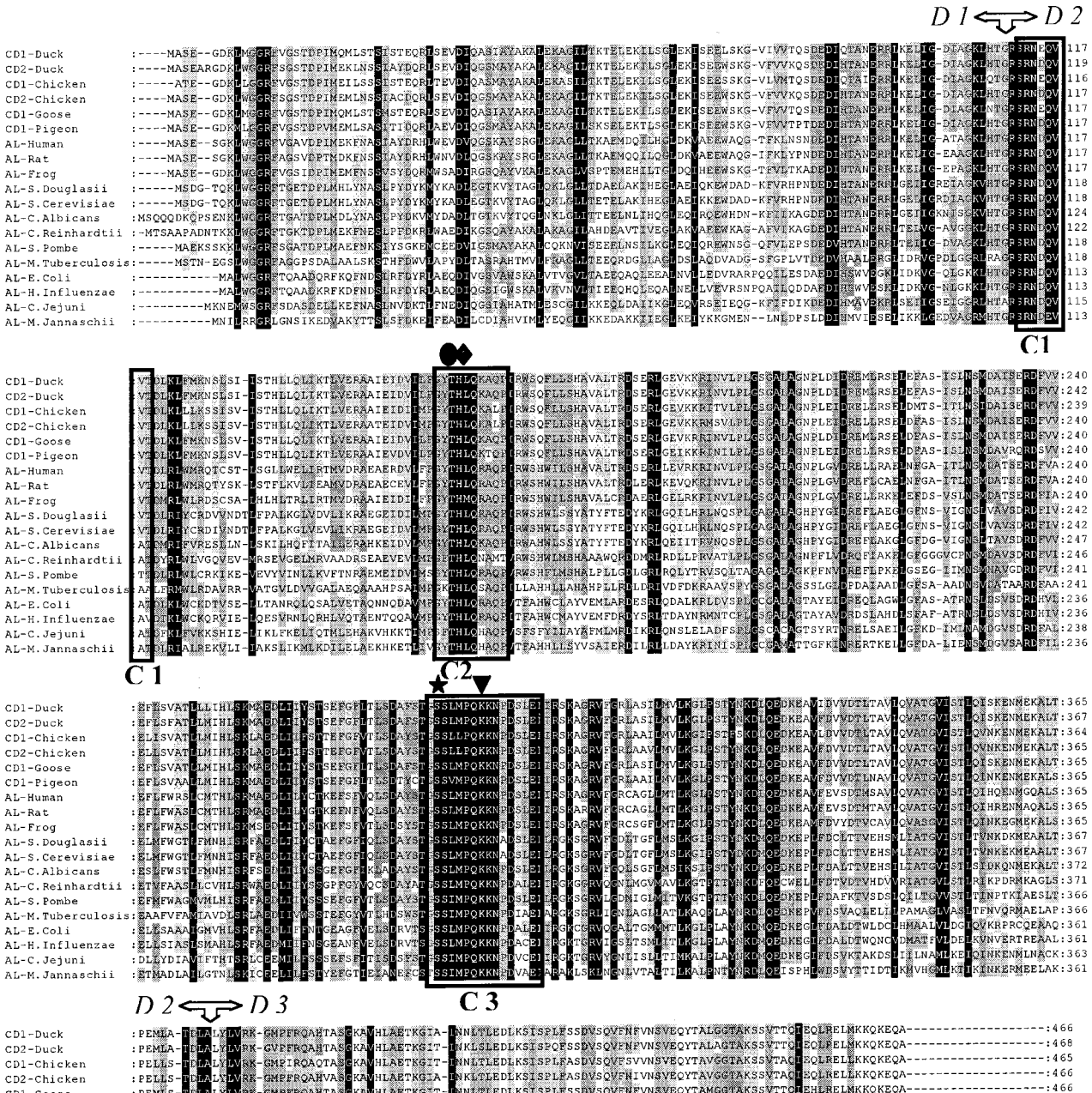

FIGURE 1: Comparison of the available δ crystallin and ASL amino acid sequences. Amino acid residues that show 100%, ≥80%, or ≥60% conservation are shaded in black, dark gray, and light gray, respectively. The figure was prepared using the program GeneDoc (*57*). The delimitation between the three structural domains (D1−D3) is shown with arrows, while the locations of the three conserved amino acid sequences in the ASL superfamily (C1−C3) are shown with boxes. Important catalytic residues Thr 159 (●), His 160 (◆), Ser 281 (★), and Lys 287 (▼) are also indicated. Abbreviations: CD1, δ1 crystallin; CD2, δ2 crystallin; AL, argininosuccinate lyase.

For all three structures, the accessible and buried surface areas were calculated with the algorithm in the CNS package, using a probe with a radius of 1.4 Å (*43*). This algorithm calculates buried surface area by summing the accessible surface area for each monomer and subtracting from this the accessible surface area of the oligomer. PROCHECK (*44*) was used to analyze the stereochemistry of the models. The final refinement statistics for all three models are presented in Table 2.

Amino Acid Sequence and Structural Alignments. The available δ crystallin and ASL sequences were retrieved from the SwissProt database, and CLUSTAL X (*45*) was used to

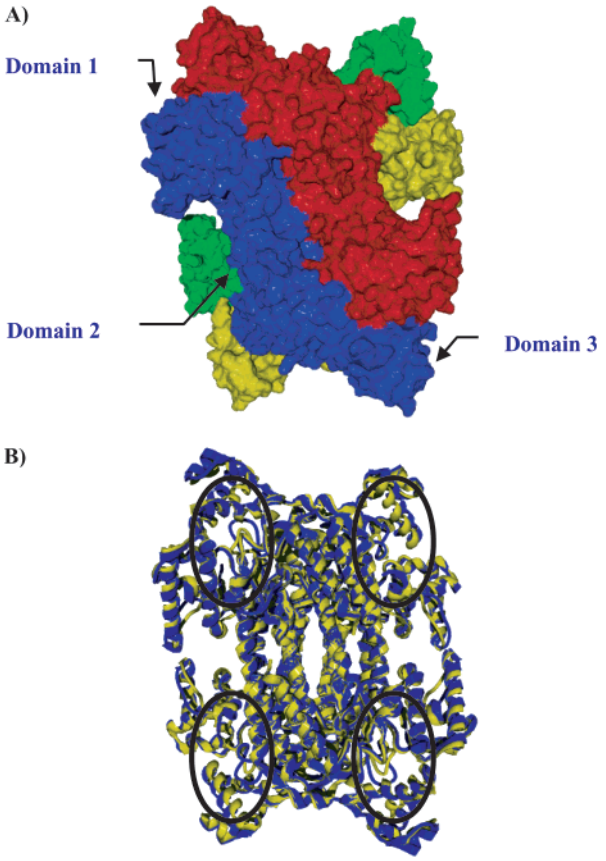

FIGURE 2: (A) Surface representation of the dδc2 tetramer. Monomers A−D are shown in yellow, blue, green, and red, respectively. The three structural domains of monomer B of dδc1 (blue) are labeled. (B) Superposition of the dδc1 (yellow) and dδc2 (blue) tetramers. The dδc1 tetramer was generated from monomers A and B present in the asymmetric unit and symmetry-related monomers C and D. The locations of the four active sites present in the tetramer are indicated by the large ovals.

perform the multiple-sequence alignment. This alignment was further improved on the basis of the structural data (Figure 1).

The structural comparison between monomers belonging to different or to the same δ crystallin structure was performed using the RIGID option in the program TURBO-FRODO (*42*). Structurally equivalent residues located in the core helices (the beginning and the end of each helix in domain 2) were selected, and an iterative least-squares fitting procedure was performed, prior to calculating the average rms deviation.

RESULTS AND DISCUSSION

Overall Fold. The wild type dδc1 and dδc2 structures (Figure 2) have the same overall architecture as that described previously for tδc1 (*20*), H91N dδc2 (*22*), H162N dδc2 (*24*), and human ASL (*23*). The N-terminus of each monomer appears to be flexible as there is generally poor quality electron density for these residues, and as a consequence, variable numbers of residues (10−19) at the N-terminal are missing in the monomers of the dδc1 and dδc2 structures. C-Terminal residues 463−466 are missing in both structures. Each monomer contains 21 helices and can be divided into three structural domains (Figures 1 and 2A). The N-terminal domain (domain 1) consists of two helix−turn−helix motifs arranged perpendicular to each other and is similar in topology to the C-terminal domain (domain 3). Nine central helices form domain 2. This is the most rigid domain in the protein as reflected by the lower-than-average *B*-factors (Table 2). Five of these central helices are clustered together in an up−down−up−down−up orientation to form a five-helix bundle. The most extensive interactions observed between monomers involve three of the five core helices from each monomer and result in the formation of the closely associated dimers, A−C and B−D. Accessible and buried surface areas confirm the importance of these interactions as the average surface area buried at the interface of the A−C (or B−D) dimer (7490 Å^2) is larger than the one buried at the A−B (or C−D) (3427 Å^2) or A−D (or B−C) (3786 Å^2) interface (see Materials and Methods). Two closely associated dimers interact to form a tetramer (Figure 2A). Each monomer contributes one helix to form a four-helix bundle at the core of the protein. The assembly of the δ crystallin tetramer as a dimer of dimers is in agreement with the experimental observation that a dimer intermediate forms during cold dissociation of ASL (*46*).

Sulfate Binding in the Active Site Region of dδc1. The location of the active site cleft in the ASL superfamily was first suggested from the wild type tδc1 structure (*20*) and

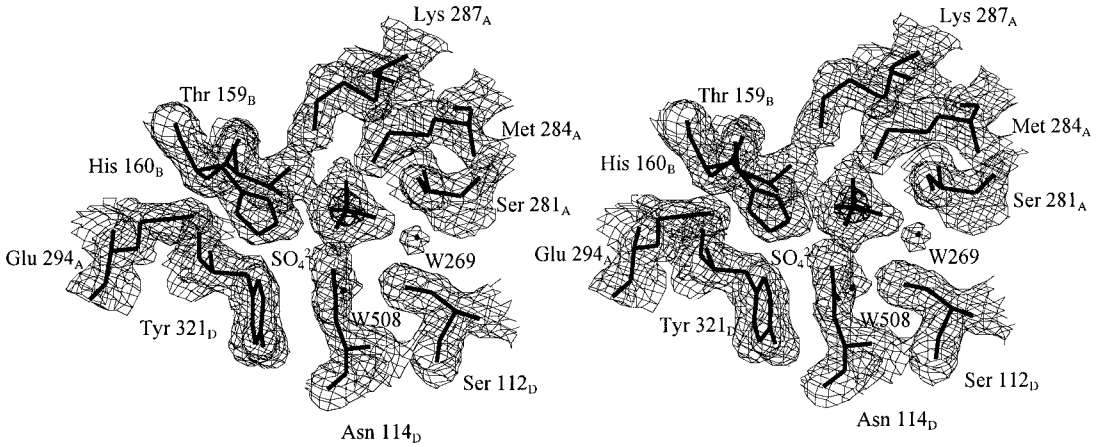

FIGURE 3: Stereoview of the electron density in the active site region of dδc1. The σ_a weighted $2|F_o| - |F_c|$ (1σ) and $|F_o| - |F_c|$ (15σ) electron density maps calculated after the SO_4^{2-} was omitted from the refinement are shown in thin and thick lines, respectively. Water molecules are denoted by W and the residue number.

Table 3: Hydrogen Bond Interactions between the Sulfate Ion, Water Molecules, and Duck δ1 Crystallin

sulfate	dδc1 residues	water molecule−protein interaction	distance (Å)
$SO_4 O_1$	Lys $287_A N_\zeta$		2.77
$SO_4 O_1$	Asn $289_A N_{\delta 2}$		3.03
$SO_4 O_2$	Ser $281_A O_\gamma$		2.61
$SO_4 O_2$	W269		2.73
	W269	Ser $281_A O_\gamma$	3.23[a]
	W269	Ser $112_D O_\gamma$	2.71[a]
$SO_4 O_3$	His $160_B N_{\epsilon 2}$		2.61
$SO_4 O_3$	W508		2.75
	W508	Asn $114_D N_{\delta 2}$	2.79[a]
$SO_4 O_4$	Thr $159_B O_{\gamma 1}$		2.77

[a] This represents the distance between water molecules W269 and W508, and residues Ser 281 and Ser 112, and Asn 114, respectively.

then confirmed by structural studies on fumarase C (*25*, *26*, *47*) and H162N dδc2 (*24*). In the ASL superfamily, there are three regions of conserved amino acid sequences denoted C1, C2, and C3, and comprised of residues 112−119, 157−166, and 280−294, respectively (Figure 1). These regions are far apart in the structure of the monomer but cluster together in the tetramer to form four independent active sites (Figure 2B). Each of the three monomers that make up an active site contributes a different conserved region. A sulfate ion has been located in the active site region of dδc1 (Figure 3). This ion interacts either directly or via a water molecule with conserved amino acid residues His 160, Thr 159, Ser 281, Lys 287, Asn 289, Ser 112, and Asn 114 (Table 3). (Please note that dδc1 and tδc1 are enzymatically inactive and therefore do not have an active site. For the purposes of the comparisons presented in this paper, the region in δc1 that is structurally homologous to the active site of dδc2 is termed the "active site region".)

His 160 interacts directly with the sulfate ion. This histidine is found in conserved region C2 and has been proposed to act as the catalytic base in the enzymatic mechanism by abstracting a proton from the C_β of the substrate either directly (*20*, *22*) or through a water molecule (*25*). Asn 289 and Asn 114 interact directly and via a water molecule with the sulfate ion, respectively (Table 3). These residues belong to conserved regions C3 and C1, respectively, and have been suggested to be involved in substrate binding (*24*, *31*). The O_2 sulfate oxygen also interacts via a water molecule with the O_γ atom of Ser 112. This residue is part of conserved region C1 and has been suggested to play a structural role in δ crystallin (*24*, *31*) and a catalytic one in fumarase C (*25*). Lys 287 and Ser 281 belong to conserved region C3 and interact directly with the sulfate. Lys 287 is the only positively charged residue in the active site region and is thought to be responsible for stabilization of the carbanion intermediate (*20*, *21*). Ser 281 has also been shown to be essential for catalysis (*31*). Chakraborty et al. (*31*) proposed that Ser 281 plays a structural role in maintaining the conformation of the loop comprised of residues 280−290 (280's loop) of conserved region C3, while Thr 159 (conserved region C2) affects catalysis by influencing the conformation of the adjacent His 160 or the protein−substrate interactions. The significance of the sulfate ion present in the active site, the conformational changes observed, and the implications for catalysis are discussed below.

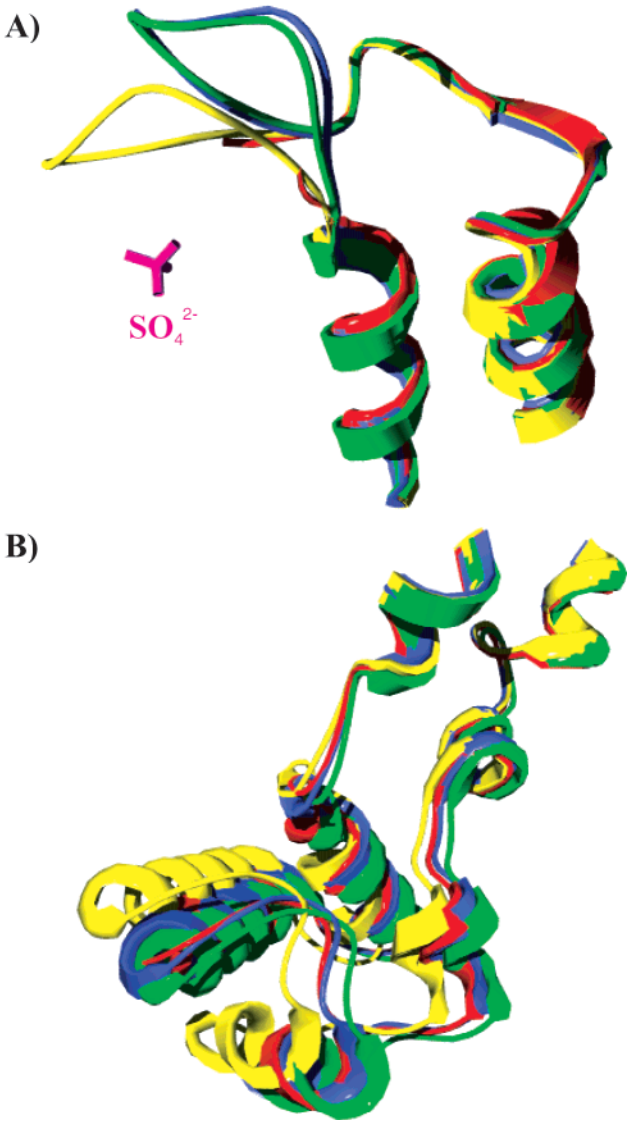

FIGURE 4: Superposition of dδc1 (yellow), tδc1 (green), dδc2 (blue), and H162N dδc2 (red) showing a closeup of the conformational changes observed in (A) the 280's loop (residues 255−300) and (B) domain 3 (residues 357−450). In panel A, the bound sulfate found in the dδc1 structure is shown in purple. Residues 274−290 are absent from the H162N dδc2 structure (*24*) and are therefore not present in panel A.

Comparison of dδc1 with all the available δ crystallin structures identified two conformational changes that appear to be the consequence of sulfate binding (Figures 2 and 4). The C_α rms deviation plots (Figure 5) show movements of approximately 8 Å in the 280's loop (Figure 4A) and up to 4 Å for domain 3 of dδc1 (Figure 4B). The conformational changes between the different structures are clearly distinguishable from the inherent small variations present in each of the structures that was analyzed. When all four monomers belonging to the same structure are compared, some variations (<1 Å) are observed in the more flexible domains (domains 1 and 3, higher *B*-factors; see Table 2). However, the low overall C_α rms deviations (0.36−0.41 Å for 415−447 C_α atoms) between all monomers of a structure suggest that no significant intrinsic differences occur within dδc1, dδc2, or H91N or H162N dδc2. The conformational changes observed in the 280's loop and domain 3 are therefore unique

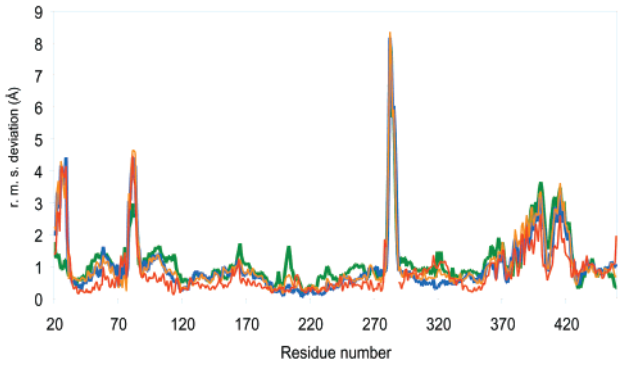

FIGURE 5: Plot of the C_α rms deviation vs residue number between monomer A of dδc1 and monomers A of tδc1 (green), dδc2 (blue), H91N dδc2 (orange), and monomer D of H162N dδc2 (red). For H162N dδc2, only one active site was occupied by substrate (*24*), and therefore, the monomer forming most of the contacts with the argininosuccinate, monomer D, was used.

to the dδc1 structure and are also independent of crystal packing interactions.

Residues in the highly flexible 280's loop (conserved region C3) are often difficult to locate in the electron density maps (*24*, *48*). In dδc1, the sulfate ion interacts directly with Ser 281, Lys 287, and Asn 289, rigidifying this loop and locking it into a specific conformation (Table 3 and Figure 4A). Examination of the temperature or *B*-factors for the 280's loop relative to those for domain 2 of the same protein clearly shows that this loop is more stable in the dδc1 structure. The average *B*-factors for the 280's loop are 26 and 44 Å^2 for dδc1 and dδc2, respectively, while the average *B*-factor for the rest of domain 2 is ~24 Å^2 in both cases.

The consequence of both sulfate binding and the conformational change of the 280's loop is that a concerted rigid body movement of residues 360−450 of domain 3 occurs (Figure 4B). This rigid body motion is supported by the fact that if domains 3 from all the structure are superimposed independent of the rest of the protein the average rms deviation for this domain is 0.7 Å. This is comparable to the average rms deviation observed for the other domains (see Figure 5). Sulfate binding affects the position of loop residues Ser 281 and Ser 282 that are hydrogen bonded to His 388 and Arg 385, respectively. These residues are part of one of the helices that make up domain 3 of a neighboring monomer. The movement of the 280's loop and the maintenance of the main chain−side chain hydrogen bonds between residues 281 and 388 and between residues 282 and 385 result in the observed rigid body motion. These structural perturbations result in dδc1 having a more compact structure, with the buried surface area in the dδc1 tetramer (29 320 Å^2) being larger than that in either dδc2 (27 613 Å^2) or tδc1 (27 812 Å^2) (see Materials and Methods).

Structural Comparison between the Enzymatically Inactive δ Crystallin Proteins dδc1 and tδc1. The original motivation for determining the structures of both enzymatically inactive and active δ crystallin was to examine differences in the structures that could help us to understand the loss of enzymatic activity in the δ1 protein. The structural differences in the 280's loop and domain 3 are however unique to dδc1 and are not found in tδc1. The tδc1 structure does not have a sulfate ion bound in the active site region, and this suggests that the conformational differences seen in the

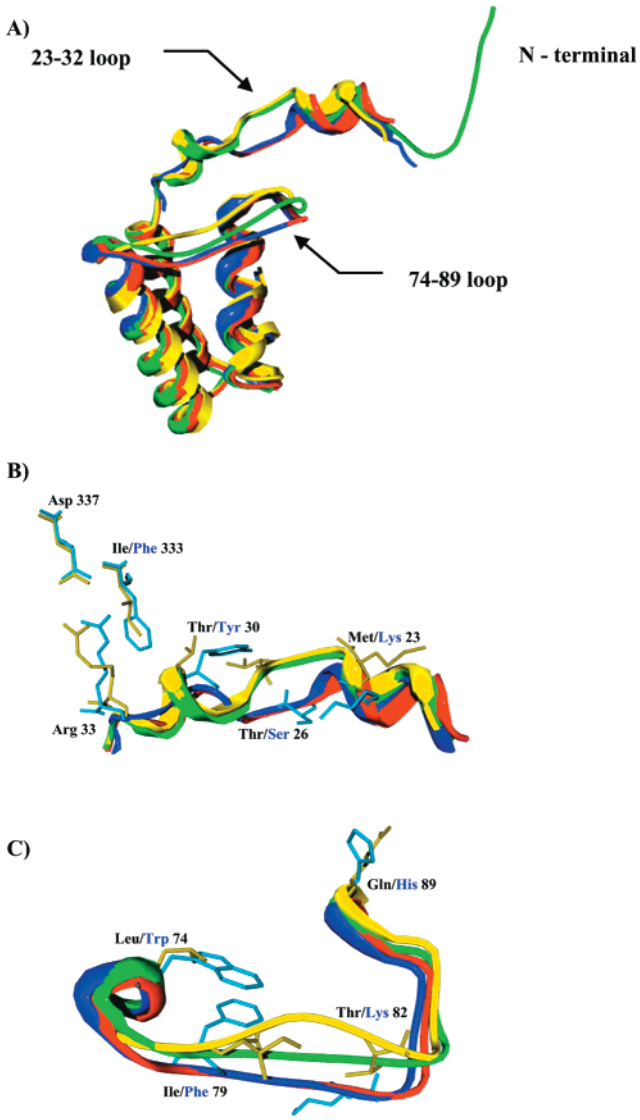

FIGURE 6: (A) Structures of dδc1 (yellow), tδc1 (green), dδc2 (blue), and H162N dδc2 (red) showing the conformational changes seen in domain 1. Closeup of the structural differences observed in the loops of residues (B) 23−32 and (C) 74−89. Amino acid residues that differ between dδc1 (yellow) and dδc2 (blue) are shown as stick representations. Each amino acid is labeled with the corresponding three-letter code, black for dδc1 and dark blue for dδc2.

280's loop and domain 3 between dδc1 and tδc1 could also occur in dδc2. The effect such a conformational change may have on the catalytic mechanism is described in more detail below.

In addition to the structural variations in the 280's loop and domain 3 of dδc1, two other significant conformational changes were observed between dδc1 and tδc1 (Figures 5 and 6A). The first involves residues in the loop of residues 74−89 and appears to be the consequence of two interspecies amino acid differences. Leu 74 and Ile 79 of dδc1 are substituted with Ser and Leu in tδc1, respectively (Figure 1). We have previously suggested that the conformational variation in this loop is a major contributing factor to the loss of enzyme activity in δ1 crystallin (*24*). The significance of this loop movement will be discussed in more detail in the context of the structural variations seen between dδc1 and dδc2.

The second conformational difference affects residues Ser 319 and Thr 320 of domain 2. In the dδc1 and dδc2 structures, the peptide bond between these two residues is in the cis conformation, while it is trans in tδc1. While we had speculated that this cis peptide bond may be important for catalysis (*22*), the presence of the cis peptide in both inactive and active duck δ crystallin would suggest a structural rather than enzymatic role for this difference. The cis peptide is probably involved in maintaining the conformation of the loop of residues 316−326, as this loop contains Tyr 321, an important substrate binding residue (*31*).

Structural Comparisons between Wild Type dδc1, dδc2, and H91N dδc2. The structures of wild type dδc1 and dδc2 were determined to eliminate any interspecies differences that may occur between tδc1 and dδc2 that could complicate our analysis and attempts to understand the structural basis for the loss of enzymatic activity in δ1 crystallin. As a consequence, the tδc1 structure has not been included in the structural comparisons presented below.

First, we examined the intraspecies structural differences that occur in the absence of bound substrate by comparing dδc1, dδc2, and the H91N dδc2 mutant. The structures of wild type dδc2 and H91N dδc2 are very similar as indicated by an rms deviation of only 0.49 Å for 448 C_α atoms. The comparison against dδc1 revealed, however, that in addition to the structural changes observed on sulfate binding discussed above, two other conformational changes occur at residues 23−32 and 74−89 (Figures 5 and 6).

The major difference between the inactive dδc1 and all dδc2 proteins is in the region of residues 23−32 (Figure 6B). There are six amino acid differences in this region, two of which are nonconservative. Lys 23 and Tyr 30 in dδc2 are replaced in dδc1 with Met and Thr, respectively (Figure 1). Despite the ∼4 Å shift in the backbone observed in this region, the salt bridge between the side chains of Arg 33 and Asp 337 is maintained in all structures. Additional van der Waals interactions also occur between Arg 33 and residue 333. The amino acid at position 333 is Ile in dδc1 and Phe in dδc2. These observations suggest that residues in the region of residues 23−32 may play a role in maintaining the structural integrity of domain 1 and the overall structure of the δ crystallin monomers as well as in substrate binding (see below and ref *24*).

The conformation of residues in the loop of residues 74−89 appears to be highly variable. Structural differences occur not only between dδc1 and tδc1 (discussed above) but also between dδc1 and different dδc2 structures (Figures 5 and 6C). Given the small number of structures available and the large variations seen in this loop, it is difficult to determine whether this region is just inherently flexible or whether a specific conformation is required for catalysis to occur. Several observations however support the latter hypothesis. First, the conformation of this loop is closer in the dδc2 wild type and mutant structures than it is in either dδc1 or tδc1. Second, the mutation of Asp 87 to Gly in ASL causes the disease argininosuccinic aciduria (*49*), and the mutation of His 89 to Asn in dδc2 results in a protein with only 10% activity (*22*). Finally, any large conformational variation in this loop will affect residues in the neighboring regions, residues 23−32 of domain 1 (Figure 6) and conserved region C1 of domain 2 (Figure 1). Both of these regions contain residues that we have shown previously to be important for substrate binding (*24*, *31*).

Structural Comparison between Wild Type dδc1 and H162N dδc2 with Bound Argininosuccinate. The structure of the enzymatically inactive H162N dδc2 mutant has been determined with substrate bound in one of its active sites (*24*). Comparison of this structure with that of dδc1 reveals that the fumarate moiety of the substrate and the sulfate ion are in comparable locations in the active site (Figure 7). Superposition of the C_α backbones reveals that in the region of the active site closest to the fumarate moiety only small conformational changes to residues 159_B and 160_B, 112_D−116_D, and 294_A−296_A occur. Larger deviations in the C_α backbones are observed in those parts of the active site involved in binding the arginine moiety of the substrate. These regions correspond to residues 23_D−32_D and 74_D−89_D of domain 1.

In the loop of residues 23−32, the structural variations between dδc1 and H162N dδc2 with bound substrate are comparable to differences seen between dδc1 and the substrate-free, wild type dδc2 (Figures 5 and 6). The consequence of this conformational variation is that residues in this region in dδc1 are further away from the arginine moiety of the substrate than in the H162N dδc2 structure. In addition, the orientation of the Thr 26 and Ser 27 side chains is changed by almost 180° (Figure 7). These differences would have a negative impact on substrate binding as residues in the loop of residues 23−32 interact with the substrate in the H162N structure. Argininosuccinate interacts directly with Ser 27 and via a water molecule with Asp 31 (Glu 31 in dδc1) (*24*).

While it is not obvious what effect residues 74−89 have on substrate binding, the identity of residue 89 appears to be important. Although the C_α atoms of residue 89 appear to be in the same position in dδc1 and H162N dδc2, the interactions of their side chains differ. In H162N dδc2, residue 89 is a histidine that interacts with the arginine moiety of the substrate via a water molecule and makes van der Waals contacts with Asp 38, Asp 87, Arg 113, and Gln 116 (*24*). In dδc1, this histidine residue is substituted with a glutamine. The poor quality of the electron density also indicates that the side chains of Gln 89, Arg 113, and Gln 116 are disordered. The conformation of the Arg 113 side chain in the dδc1 structure appears to be influenced by both the loop of residues 74−89 and the 280's loop, as this residue makes van der Vaals contacts with not only Glu 86 and Gln 89 but also Ser 282. Like Arg 113, its neighboring residues Asn 114 and Ser 112 (conserved region C1) have also been shown to be important for substrate binding (*24*, *31*) (Figure 7). The dδc1 structure supports this conclusion with Asn 114 and Ser 112 interacting via a water molecule with the sulfate ion. This structural comparison suggests that the identity and conformation of the residue at position 89 and the conformation of the loop of residues 74−89 are critical for maintaining the conformation of the residues involved in substrate binding.

These observations regarding the importance of residues 23−32 and 74−89 are consistent with our previous studies (*22*, *24*, *32*) and reinforce the hypothesis that conformational changes in domain 1 are the primary cause for loss of enzymatic activity in δ1 crystallin.

Catalytic Mechanism of the δ2 Crystallin/ASL System. The dδc1 structure with bound sulfate and the hypothesis that

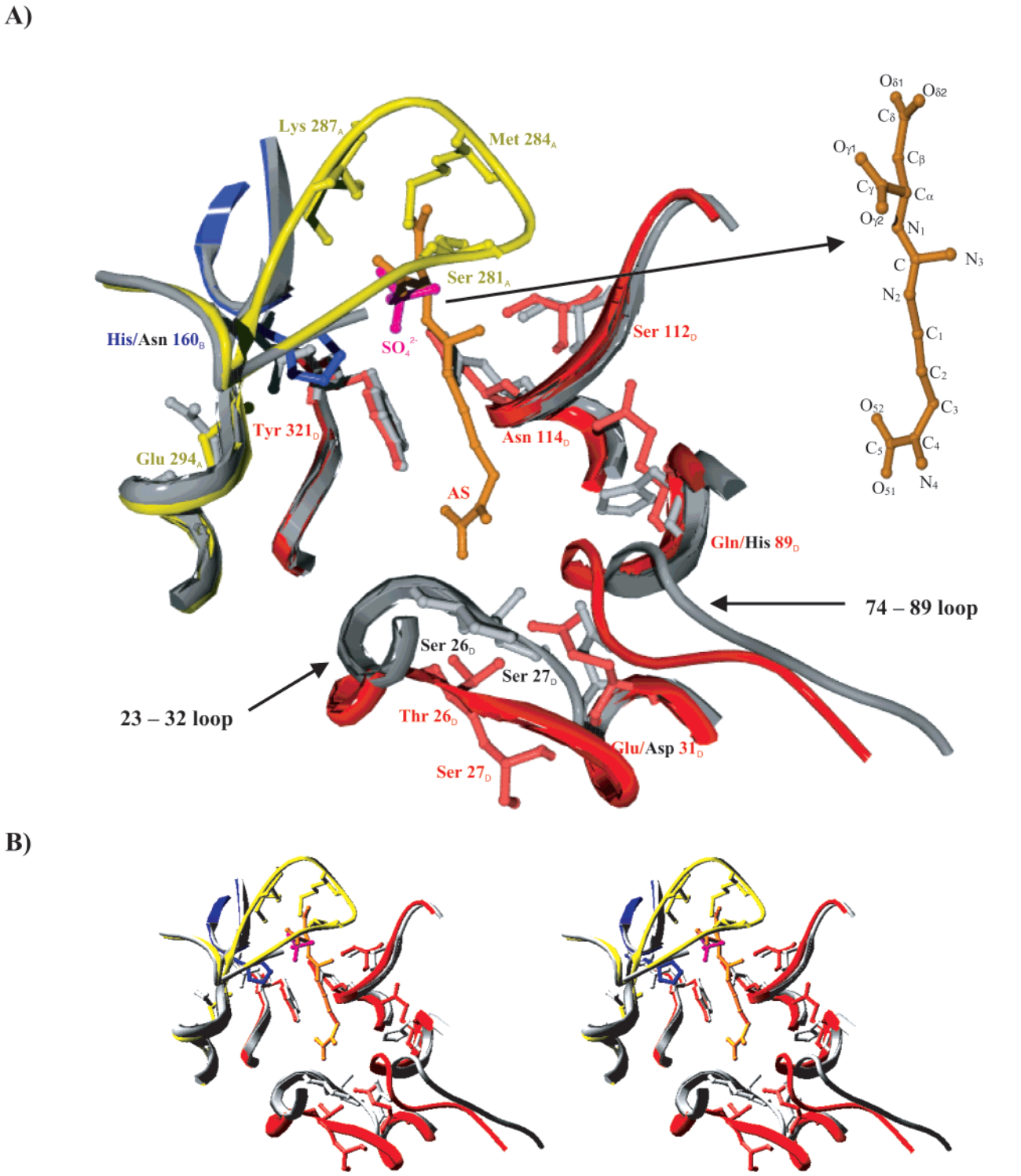

FIGURE 7: (A) Closeup of the active site region of dδc1 and H162N dδc2. The backbone and residue side chains corresponding to dδc1 are colored according to their monomer of origin (as in Figure 2A). The H162N dδc2 backbone and residue side chains are shown in gray. The sulfate anion (SO_4^{2-}) is shown in pink and the argininosuccinate substrate (AS) in orange. The inset shows the argininosuccinate with all atoms labeled. (B) Stereoview of the image shown in panel A emphasizing the depth of the active site region.

the observed structural changes in the 280's loop and domain 3 could also occur in dδc2 prompted a re-examination of the catalytic mechanism of the protein. The structural alignment of dδc1 and H162N dδc2 clearly shows that the sulfate ion can be superimposed with one of the carboxylate groups of the fumarate moiety of the substrate (Figure 7A). While the 280's loop is not visible in the H162N dδc2 structure with substrate bound, it is seen in the dδc1 structure. Duck δ1 crystallin therefore offers insight into the potential conformation of this loop in the presence of bound substrate. Additionally, the conformation of the 280's loop in dδc1 is different from that found in any of the uncomplexed δ crystallin structures (tδc1, dδc2, and H91N dδc2) (Figures 4A and 5). If substrate binding in dδc2 induces the same conformational changes of the 280's loop as that observed in dδc1, then only a slight rearrangement of the fumarate

moiety or the side chain of Met 284 would be required to eliminate steric hindrance (Figure 7A). The electron density for the fumarate moiety is not well-defined in the H162N dδc2 structure, suggesting that such a conformational change would be possible. The interactions seen in dδc1 between the sulfate and the 280's loop suggest for the first time an interaction between argininosuccinate and Ser 281. When the substrate is modeled in the wild type dδc2 structure, the O_γ atom of Ser 281 is 8.8 and 7.7 Å from the N_1 and C_α atoms of the substrate, respectively. With the conformational change of the 280's loop seen in the dδc1 structure, these distances are reduced to 3.9 and 2.85 Å, respectively. The distance between the O_γ atom of Ser 281 and the N_1 atom of the substrate could also be shortened with a reorientation of the side chain of Ser 281. The conformational change and flexibility of the 280's loop allow it to form a "lid" over the active site (Figure 7B), sequestering the substrate from the solvent. Ser 281 comes within hydrogen bonding distance of the scissile bond of the substrate and is in a position to act as the catalytic acid.

In addition to Ser 281 being in the proximity of the sulfate, there are other observations supporting the hypothesis that this residue may play an important role in the enzymatic mechanism of dδc2/ASL. The reaction occurs with trans stereochemistry (*50*, *51*), and Ser 281 is on the opposite side of the substrate with respect to putative catalytic base His 160. Kinetic isotope studies show that the last step of the reaction, the cleavage of the N_1-C_α bond of the substrate in which a proton is donated to N_1, is the rate-limiting step (*51*). These data suggest that the acid catalyst may be a weak acid, making a serine residue a more attractive candidate for the acid catalyst than either asparate or glutamate as each of these residues is more likely to give up their proton. Site-directed mutagenesis studies in dδc2 have also shown that this residue is important in catalysis, as substitution of Ser 281 with Ala resulted in an enzymatically inactive protein (*31*). Ser 281 also belongs to conserved sequence C3 and is one of the very few residues in this region that are strictly conserved in the entire ASL superfamily (Figure 1). Finally, while the suggestion of a serine as the catalytic acid is uncommon, it is not novel as serine residues have been suggested to be proton donors in the photosynthetic reaction centers of both *Rhodopseudomonas* (*52*) and *Rhodobacter sphaeroides* (*53*), in the flavoprotprotein MurB (*54*), and in lecithin-cholesterol acyltransferase (*55*).

Intriguingly, in the structure of dδc1, Thr 159 is in close proximity to Lys 287 and the sulfate ion. Thr 159 belongs to conserved region C2 and is highly conserved across the superfamily with the only sequence variations being in *Helicobacter pylori* and *Synecocystis* sp. adenylosuccinate lyases where it is replaced with serine (*48*). A short hydrogen bond (2.52 Å) exists between the $O_{\gamma 1}$ atom of Thr 159 and the N_ζ atom of Lys 287, suggesting that Lys 287 could lower the pK_a of the hydroxyl group of Thr 159 (Figure 3). The $O_{\gamma 1}$ atom of Thr 159 is also within hydrogen bonding distance of the O4 atom the of sulfate ion (Table 3). In the wild type dδc2 structure, the side chain of Thr 159 is in a different orientation such that the $O_{\gamma 1}$ atom does not hydrogen bond with Lys 287 but is 3.47 Å from the C_β atom of the argininosuccinate substrate (as modeled in H162N dδc2). These observations suggest that Thr 159 could have a role in base catalysis, a hypothesis that is supported by the loss of enzymatic activity in the Thr 159 to Val dδc2 mutant (*31*) and the lack of strict conservation of His 160 across the superfamily. While His 160, given its charge relay interaction with Glu 294, is the more attractive base catalyst, its lack of conservation across the superfamily is puzzling given the similarity of the three-dimensional structures of the members of the superfamily and the expectation that the catalytic machinery will be conserved. A comprehensive structural comparison of all members of the superfamily in the presence and absence of bound inhibitors is in progress and should shed further light on the role of Ser 281, His 160, and Thr 159 in the catalytic mechanism.

CONCLUSIONS

The structural comparisons presented here suggest that a significant conformational change in the 280's loop and rigid body movement of domain 3 may occur on substrate binding. In addition, the results suggest for the first time that strictly conserved residue Ser 281 could be the acid catalyst and raise questions regarding the role of His 160, the putative catalytic base. These hypotheses are however based on the structural comparison of the inactive dδc1−sulfate and H162N dδc2−substrate complexes. Structures of wild type dδc2 with inhibitor bound and/or of an inactive dδc2 mutant with substrate bound (in which the mutation does not significantly affect the substrate binding capacity) will be determinant in confirming whether Ser 281 is the acid catalyst and what role His 160 has in the catalytic mechanism.

ACKNOWLEDGMENT

We thank Anita Chakraborty for help with crystallization and data collection on wild type dδc2 and Lori A. Maggisano for optimizing the purification protocol for dδc1.

REFERENCES

1. Piatigorsky, J. (1981) *Biochemistry 20*, 6427−31.
2. Delaye, M., and Tardieu, A. (1983) *Nature 302*, 415−7.
3. Piatigorsky, J. (1989) *FASEB J. 3*, 1933−40.
4. Piatigorsky, J., Kantorow, M., Gopal-Srivastava, R., and Tomarev, S. I. (1994) *EXS 71*, 241−50.
5. Piatigorsky, J., O'Brien, W. E., Norman, B. L., Kalumuck, K., Wistow, G. J., Borras, T., Nickerson, J. M., and Wawrousek, E. F. (1988) *Proc. Natl. Acad. Sci. U.S.A. 85*, 3479−83.
6. Janssens, H., and Gehring, W. J. (1999) *Dev. Biol. 207*, 204−14.
7. Piatigorsky, J. (1998) *Prog. Retinal Eye Res. 17*, 145−74.
8. Gehring, W. J., and Ikeo, K. (1999) *Trends Genet. 15*, 371−7.
9. Mori, M., Matsubasa, T., Amaya, Y., and Takiguchi, M. (1990) *Prog. Clin. Biol. Res. 344*, 683−99.
10. O'Brien, W. E., McInnes, R., Kalumuck, K., and Adcock, M. (1986) *Proc. Natl. Acad. Sci. U.S.A. 83*, 7211−5.
11. Lee, H. J., Chiou, S. H., and Chang, G. G. (1992) *Biochem. J. 283*, 597−603.
12. Chiou, S. H., Lee, H. J., Chu, H., Lai, T. A., and Chang, G. G. (1991) *Biochem. Int. 25*, 705−13.
13. Kondoh, H., Araki, I., Yasuda, K., Matsubasa, T., and Mori, M. (1991) *Gene 99*, 267−71.
14. Chiou, S. H., Hung, C. C., and Lin, C. W. (1992) *Biochim. Biophys. Acta 1160*, 317−24.
15. Barbosa, P., Wistow, G. J., Cialkowski, M., Piatigorsky, J., and O'Brien, W. E. (1991) *J. Biol. Chem. 266*, 22319−22.
16. Woods, S. A., Schwartzbach, S. D., and Guest, J. R. (1988) *Biochim. Biophys. Acta 954*, 14−26.

17. Woods, S. A., Miles, J. S., Roberts, R. E., and Guest, J. R. (1986) *Biochem. J. 237*, 547−57.
18. Stone, R. L., Zalkin, H., and Dixon, J. E. (1993) *J. Biol. Chem. 268*, 19710−6.
19. Williams, S. E., Woolridge, E. M., Ransom, S. C., Landro, J. A., Babbitt, P. C., and Kozarich, J. W. (1992) *Biochemistry 31*, 9768−76.
20. Simpson, A., Bateman, O., Driessen, H., Lindley, P., Moss, D., Mylvaganam, S., Narebor, E., and Slingsby, C. (1994) *Nat. Struct. Biol. 1*, 724−34.
21. Saribas, A. S., Schindler, J. F., and Viola, R. E. (1994) *J. Biol. Chem. 269*, 6313−9.
22. Abu-Abed, M., Turner, M. A., Vallée, F., Simpson, A., Slingsby, C., and Howell, P. L. (1997) *Biochemistry 36*, 14012−22.
23. Turner, M. A., Simpson, A., McInnes, R. R., and Howell, P. L. (1997) *Proc. Natl. Acad. Sci. U.S.A. 94*, 9063−8.
24. Vallée, F., Turner, M. A., Lindley, P. L., and Howell, P. L. (1999) *Biochemistry 38*, 2425−34.
25. Weaver, T. M., Levitt, D. G., Donnelly, M. I., Stevens, P. P., and Banaszak, L. J. (1995) *Nat. Struct. Biol. 2*, 654−62.
26. Weaver, T., and Banaszak, L. (1996) *Biochemistry 35*, 13955−65.
27. Weaver, T., Lees, M., Zaitsev, V., Zaitseva, I., Duke, E., Lindley, P., McSweeny, S., Svensson, A., Keruchenko, J., Keruchenko, I., Gladilin, K., and Banaszak, L. (1998) *J. Mol. Biol. 280*, 431−42.
28. Garrard, L. J., Bui, Q. T., Nygaard, R., and Raushel, F. M. (1985) *J. Biol. Chem. 260*, 5548−53.
29. Lee, H. J., Chiou, S. H., and Chang, G. G. (1993) *Biochem. J. 293*, 537−44.
30. Patejunas, G., Barbosa, P., Lacombe, M., and O'Brien, W. E. (1995) *Exp. Eye Res. 61*, 151−4.
31. Chakraborty, A. R., Davidson, A., and Howell, P. L. (1999) *Biochemistry 38*, 2435−43.
32. Sampaleanu, L. M., Davidson, A. R., Graham, C., Wistow, G. J., and Howell, P. L. (1999) *Protein Sci. 8*, 529−37.
33. Otwinowski, Z., and Minor, W. (1997) *Methods Enzymol. 276*, 307−26.
34. Navaza, J. (1994) *Acta Crystallogr. A50*, 157−63.
35. Brunger, A. T., Adams, P. D., Clore, G. M., DeLano, W. L., Gros, P., Grosse-Kunstleve, R. W., Jiang, J. S., Kuszewski, J., Nilges, M., Pannu, N. S., Read, R. J., Rice, L. M., Simonson, T., and Warren, G. L. (1998) *Acta Crystallogr. D54*, 905−21.
36. Adams, P. D., Pannu, N. S., Read, R. J., and Brunger, A. T. (1997) *Proc. Natl. Acad. Sci. U.S.A. 94*, 5018−23.
37. Pannu, N. S., Murshudov, G. N., Dodson, E. J., and Read, R. J. (1998) *Acta Crystallogr. D54*, 1285−94.
38. Wang, B. C. (1985) *Methods Enzymol. 115*, 90−112.
39. Rice, L. M., and Brunger, A. T. (1994) *Proteins 19*, 277−90.
40. Brunger, A. T., Adams, P. D., and Rice, L. M. (1998) *Curr. Opin. Struct. Biol. 8*, 606−11.
41. Read, R. J. (1986) *Acta Crystallogr. A42*, 140−9.
42. Roussel, A., and Cambillau, C. (1991) *TURBO-FRODO*, Silicon Graphics, Mountain View, CA.
43. Lee, B., and Richards, F. M. (1971) *J. Mol. Biol. 55*, 379−400.
44. Laskowski, R. A., MacArthour, M. W., Moss, D. S., and Thornton, J. M. (1993) *J. Appl. Crystallogr. 26*, 283−91.
45. Jeanmougin, F., Thompson, J. D., Gouy, M., Higgins, D. G., and Gibson, T. J. (1998) *Trends Biochem. Sci. 23*, 403−5.
46. Schulze, I. T., Lusty, C. J., and Ratner, S. (1970) *J. Biol. Chem. 296*, 6313−9.
47. Weaver, T., Lees, M., and Banaszak, L. (1997) *Protein Sci. 6*, 834−42.
48. Toth, E. A., and Yeates, T. O. (2000) *Struct. Folding Des. 8*, 163−74.
49. Walker, D. C., McCloskey, D. A., Simard, L. R., and McInnes, R. R. (1990) *Proc. Natl. Acad. Sci. U.S.A. 87*, 9625−9.
50. Hoberman, H. D., Havir, E. A., Rochovansky, O., and Ratner, S. (1965) *J. Biol. Chem. 239*, 3818−20.
51. Wu, C. Y., Lee, H. J., Wu, S. H., Chen, S. T., Chiou, S. H., and Chang, G. G. (1998) *Biochem. J. 333*, 327−34.
52. Leibl, W., Sinning, I., Ewald, G., Michel, H., and Breton, J. (1993) *Biochemistry 32*, 1958−64.
53. Paddock, M. L., McPherson, P. H., Feher, G., and Okamura, M. Y. (1990) *Proc. Natl. Acad. Sci. U.S.A. 87*, 6803−7.
54. Benson, T. E., Walsh, C. T., and Massey, V. (1997) *Biochemistry 36*, 796−805.
55. Vohl, M. C., Neville, T. A., Kumarathasan, R., Braschi, S., and Sparks, D. L. (1999) *Biochemistry 38*, 5976−81.
56. Kawata, Y., Tamura, K., Kawamura, M., Ikei, K., Mizobata, T., Nagai, J., Fujita, M., Yano, S., Tokushige, M., and Yumoto, N. (2000) *Eur. J. Biochem. 267*, 1847−57.
57. Nicholas, K. B., Nicholas, H. B., Jr., and Deerfield, D. W. (1997) http://www.ebi.ac.uk/embnet.news, pp 4−14.

BI002272K